Frontiers in Bioscience Landmark

Front. Biosci. (Landmark Ed) **2026**; 31(6): 50766
https://doi.org/10.31083/FBL50766

Original Research

Reshaping the Immune Microenvironment by Targeting DKK1 to Enhance Combination Immunotherapy Efficacy in Head and Neck Squamous Cell Carcinoma

Fei Wang[1], Minzhu Yan[1], Xuelin Dong[2], Zhijun Zhang[2], Pin Dong[1,*], Xinwei Chen[1,*]

[1]Department of Otolaryngology, Head and Neck Surgery, Shanghai General Hospital of Nanjing Medical University, 200080 Shanghai, China
[2]Department of Otolaryngology, Head and Neck Surgery, Shuguang Hospital Affiliated to Shanghai University of Traditional Chinese Medicine, 200021 Shanghai, China
*Correspondence: dongpin64@aliyun.com (Pin Dong); xinwei.chen@shgh.cn (Xinwei Chen)
Academic Editor: Qingping Dou
Submitted: 5 February 2026 Revised: 8 April 2026 Accepted: 30 April 2026 Published: 17 June 2026

Abstract

Background: Head and neck squamous cell carcinoma (HNSCC) is a common malignancy with high morbidity and mortality. Despite advances in immunotherapy, including the advent of immune checkpoint inhibitors (ICIs) targeting programmed cell death protein 1 (PD-1)/programmed cell death ligand 1 (PD-L1), only a subset of patients achieves significant benefit. This study aimed to evaluate the prognostic significance of Dickkopf-related protein 1 (DKK1), a potential modulator of the tumor immune microenvironment (TME), and to assess the therapeutic impact of combining DKK1 inhibition with ICIs. **Methods**: Data from The Cancer Genome Atlas (TCGA) and a clinical cohort of 62 patients with HNSCC from Shanghai General Hospital were used to analyze DKK1 expression and its association with prognosis and immune cell infiltration. Tumor immune organoids were constructed by co-culturing tumor and immune cells from patient samples to mimic the TME and evaluate the effects of anti-DKK1 therapy. A preclinical mouse model using the MOC2 (mouse oral carcinoma 2) cell line was also used to test the therapeutic efficacy of combined anti-DKK1 and anti-PD1 treatment. Immune cell composition was analyzed using immunohistochemistry, immunofluorescence, and flow cytometry. **Results**: High DKK1 expression was found to correlate with poor patient prognosis and an immunosuppressive TME, characterized by reduced CD8+ T cell infiltration and increased myeloid-derived suppressor cells (MDSCs). In tumor immune organoids, anti-DKK1 treatment reduced organoid growth. *In vivo*, combined anti-DKK1 and anti-PD1 treatment led to significantly greater tumor growth inhibition compared to monotherapies, increased CD8+ T cell activity, and decreased MDSC levels, thereby creating an immune-stimulatory environment. **Conclusions**: DKK1 drives immune suppression in HNSCC and represents a promising therapeutic target. Tumor immune organoids offer a robust platform for studying tumor-immune interactions and evaluating combination immunotherapies. Combining anti-DKK1 and anti-PD1 treatment approaches has the potential to enhance antitumor immunity and improve outcomes in patients with HNSCC.

Keywords: squamous cell carcinoma of head and neck; Dickkopf-related protein 1; tumor microenvironment; immune checkpoint inhibitors

1. Background

Head and neck squamous cell carcinoma (HNSCC) is one of the most common malignancies globally, characterized by a high degree of morbidity and mortality [1,2]. Despite advancements in treatment, including surgery, radiotherapy, and chemotherapy, the prognosis for patients with HNSCC remains poor, particularly in those with advanced disease [3–5]. New therapeutic options have become available to patients through the rapid development of new forms of immunotherapy, including immune checkpoint inhibitors (ICIs) targeting the programmed cell death protein 1 (PD-1) and its ligand (PD-L1) [6,7]. However, ICIs response rates are limited [8,9], with only a subset of patients benefiting from these treatments. Identifying novel biomarkers that can predict therapeutic response and modulate the immune microenvironment is critical for improving outcomes in HNSCC.

The tumor microenvironment (TME) is increasingly recognized as a critical factor influencing the effectiveness of cancer immunotherapy [10]. Immunosuppressive cells, such as myeloid-derived suppressor cells (MDSCs), regulatory T cells (Tregs), and tumor-associated macrophages (TAMs), contribute to the resistance against ICIs by inhibiting cytotoxic T cell responses [11–13]. Efforts to target components of the TME with the goal of counteracting such immunosuppression have shown promise as a means of enhancing immune responses and improving ICI efficacy [14]. One such target is Dickkopf-related protein 1 (DKK1), a secreted glycoprotein and antagonist of the Wnt/β-catenin signaling pathway [15,16]. DKK1 has been implicated in the establishment of an immunosuppressive TME through its ability to alter the migration and activity of MDSCs [17,18], which are a heterogeneous population of immunosuppressive cells crucial for dampening antitumor immunity [19,20]. Through this pathway, DKK1

can foster an immunosuppressive TME, reducing the efficacy of immune-based therapies and promoting tumor progression [21]. In addition to its effects on MDSCs, recent studies have suggested that DKK1 may also regulate other immune components within the TME, including dendritic cells, macrophages, and T-cell-associated antitumor responses. These findings indicate that DKK1 may function as a broader immunomodulatory factor in cancer progression and immune evasion [22]. Given its immunosuppressive function, DKK1 offers promise as a novel therapeutic target when seeking to counteract immune suppression with the TME, especially in combination with ICI treatment. DKK1 has also recently been suggested to play a role in resistance to radiotherapy [23], emphasizing its broad potential clinical relevance. However, the specific role that DKK1 plays in the modulation of immunotherapy responses in HNSCC remains unclear. Importantly, DKK1-targeted therapy has already entered clinical evaluation. The anti-DKK1 monoclonal antibody DKN-01 has been tested in gastroesophageal adenocarcinoma, including in combination with PD-1 blockade, highlighting the translational potential of DKK1-directed strategies in cancer therapy [24,25].

Tumor-derived organoids have revolutionized cancer research in recent years, providing advanced *in vitro* models suitable for more nuanced analyses of tumor biology and drug responses [26]. As an application of organoid-based technologies, tumor immune organoids incorporate both tumor cells and immune components, allowing researchers to replicate the intricate interactions within the TME with greater fidelity [27]. These organoids offer a unique platform for investigating the immunomodulatory effects of DKK1 inhibition and its potential to synergize with ICIs in HNSCC. By mimicking the native tumor-immune landscape, tumor immune organoids facilitate precise modeling of therapeutic interventions, accelerating the development of personalized treatment strategies [28].

To address the gaps in knowledge outlined above, this study was devised with the aim of characterizing the role of DKK1 in shaping the immune landscape of HNSCC and evaluating its potential as a therapeutic target. We evaluated the prognostic significance of DKK1 expression in HNSCC using data from The Cancer Genome Atlas (TCGA) and validated our findings in a clinical cohort. To further explore the therapeutic relevance of DKK1, we evaluated the effects of anti-DKK1 therapy, both alone and in combination with anti-PD1, in preclinical HNSCC models, including patient-derived tumor immune organoids. Together, our findings provide compelling evidence for targeting DKK1 to mitigate immune suppression and enhance the efficacy of ICIs in HNSCC.

2. Methods

2.1 Data Source and Bioinformatic Analysis

Data from The TCGA database were used to evaluate DKK1 expression in HNSCC and assess its association with patient prognosis [29]. Expression data for DKK1 and clinical characteristics were retrieved, including overall survival (OS) data. Kaplan-Meier survival analysis was conducted to examine the association between DKK1 expression levels (categorized as high or low) and OS outcomes [30]. Patients in the TCGA cohort were divided into high- and low-DKK1 expression groups according to the median value of DKK1 expression. In addition, TCGA data were used to assess immune checkpoint-related gene expression in the DKK1-high and -low groups in an effort to investigate the relationship between this gene and the immune microenvironment. Single-cell RNA sequencing (scRNA-seq) data from the GSE103322 dataset [31] were additionally analyzed to gain further insights into DKK1 expression across different cell populations within the HNSCC TME. Cell clustering analysis was visualized using t-SNE plots, and DKK1 expression was examined across the identified cell types.

2.2 Clinical HNSCC Cohort

A cohort of 62 patients diagnosed with HNSCC from Shanghai General Hospital were enrolled in this study. The characteristics of the 62 patients HNSCC cohort are summarized in Table 1. Tumor samples were collected, and patients were grouped based on DKK1 expression, determined via immunohistochemistry (IHC), into DKK1-low and DKK1-high groups. DKK1 immunohistochemical staining was evaluated using the H-score method. Briefly, the H-score was calculated based on both staining intensity and the percentage of positive tumor cells, and patients were classified into high- and low-expression groups according to the median H-score. Clinical outcomes were compared between the two groups, with a primary focus on patient OS. This study was conducted in accordance with the ethical principles of the Declaration of Helsinki and approved by the Institutional Review Board of Shanghai General Hospital (2020KY144), with informed consent having been obtained from all participants.

2.3 Immunohistochemistry and Immunofluorescence

IHC-based detection of DKK1 expression was performed on formalin-fixed, paraffin-embedded HNSCC tissue sections [32]. After deparaffinization and rehydration, sections were subjected to antigen retrieval, followed by incubation with a primary antibody against DKK1 (Abcam, ab61034, 1:100) at 4 °C overnight. After washing, sections were incubated with an HRP-conjugated secondary antibody for 1 h at room temperature, followed by signal development. Immunofluorescence staining was conducted to detect immune cell markers in the TME [33,34], including CD8 (BioLegend, 301002), PD-L1 (Cell Signaling

Table 1. Characteristics of 62 patients HNSCC cohort.

Variable	Category	n (%)
Total patients		62
Age, years	Median (range)	61 (41–79)
Sex	Male	61 (98.4)
	Female	1 (1.6)
T stage	T1	18 (29.0)
	T2	11 (17.7)
	T3	27 (43.5)
	T4	6 (9.7)
N stage	N0	15 (24.2)
	N1	14 (22.6)
	N2	24 (38.7)
	N3	9 (14.5)
M stage	M0	59 (95.2)
	M1	3 (4.8)
Tumor differentiation	Low	23 (37.1)
	Medium	5 (8.1)
	High	34 (54.8)
HPV status	Positive	14 (22.6)
	Negative	48 (77.4)
Smoking history	Yes	49 (79.0)
	No	13 (21.0)
Treatment history before tissue collection	No prior antitumor treatment	62 (100.0)

Technology, 13684), CD15 (Abcam, ab135377), and CD14 (Abcam, ab314062). Primary antibodies were incubated at 4 °C overnight, followed by incubation with fluorophore-conjugated secondary antibodies for 1 h at room temperature in the dark. Fluorescently labeled secondary antibodies were used, and images were acquired to capture patterns of immune cell infiltration patterns. Quantification of stained cells was achieved by counting positive cells per field of view (FOV).

2.4 Construction of Tumor Immune Organoids

HNSCC tumor immune organoids were generated by co-culturing tumor cells and immune cells isolated from patient tumor samples. Primary tumor cells and immune cells used for organoid construction were freshly isolated from surgical specimens of HNSCC patients and were not passaged long-term *in vitro*. Tumor tissues were enzymatically dissociated into single-cell suspensions, and CD45+ immune cells were enriched through a magnetic-activated cell sorting (Miltenyi Biotec) approach. The post-sorting purity of CD45+ cells was assessed by flow cytometry and was typically greater than 90%. Tumor immune organoids were generated from 10 independent HNSCC patient samples. For each patient, experiments were performed with three technical replicates per condition. Tumor cells and immune cells were mixed at a 3:1 ratio and co-cultured for 24–36 hours treated in the presence of anti-DKK1 (Sino Biological,10170-R0155) or an isotype control antibody. Tumor cells were then embedded in Matrigel droplets in 48-well plates. Organoids were subsequently cultured in advanced DMEM/F12 medium supplemented with B27, N2, and immune-supportive factors, including IL-2, at 37 °C with 5% CO_2. After 7–10 days of culture, organoids were analyzed. For statistical analysis, each patient was treated as an independent biological replicate.

2.5 Mouse Model and Therapeutic Interventions

A subcutaneous tumor model was established in C57BL/6 mice (male, 6–8 weeks old), which were purchased from Shanghai Jiesijie Laboratory Animal Co., Ltd. (Shanghai, China; production license No. SYXK (Hu) 2022-0017). Male C57BL/6J mice were used to avoid sex-related variability in immune responses. A priori sample size estimation was performed using tumor growth inhibition as the primary outcome. Based on preliminary experiments and comparable syngeneic HNSCC mouse model studies, the expected treatment effect of combined anti-DKK1 and anti-PD1 therapy was considered large. Assuming a two-sided α of 0.05, 80% power, and an estimated standardized effect size of approximately 2.0, at least four mice per group were required. To account for biological variability and to comply with the 3Rs principle, five mice per group were used in the in vivo therapeutic experiment. The sample size was also consistent with previous publications [35]. Mice were housed under specific pathogen-free conditions at 22 ± 2 °C, $50 \pm 10\%$ humidity, with a

12:12 h light-dark cycle and free access to sterile food and water. The (mouse oral carcinoma 2) MOC2 cell line was purchased from Sunncell (Wuhan, China). Cell line authenticity was confirmed by the supplier, and the cells were routinely tested to ensure absence of mycoplasma contamination before use. After subcutaneously implanting MOC2 cells (1×10^6 cells in 100 µL PBS) in the right flank of each mouse [36], tumors were allowed to grow to a measurable size. Mice were included for treatment allocation only when tumors became measurable and when animals showed no signs of poor general health before treatment initiation. The mice were randomized to four treatment groups: isotype control, anti-PD1 treatment, anti-DKK1 treatment, and combination therapy (anti-DKK1 + anti-PD1). Each mouse was given a unique number from 1 to 20, and a random number was generated for each mouse using Excel (RAND function). The mice were then sorted in ascending order of the random numbers. Twenty mice were randomly assigned into four groups (n = 5 per group). The anti-PD1 (Bio X Cell, BE0146) and anti-DKK1 (Sino Biological, 10170-R0155) antibody treatments were administered intraperitoneally every three days following tumor establishment [17,35]. Treatment continued for a total of two weeks, after which the mice were euthanized, and tumors were harvested for analysis. Mice in the control group were instead administered an isotype control antibody (Bio X Cell, BE0090) on the same schedule. Mice were monitored every three days for tumor growth, body weight, general appearance, activity, grooming behavior, and signs of distress. All mice completed the treatment protocol without reaching humane endpoints (tumor ulceration, tumor volume >2000 mm^3, body weight loss >20%, impaired mobility, severe distress, or moribund status). The final sample size for each group was 5 mice. Tumor volume was measured every three days using calipers and calculated using the formula: volume = length $\times$ $width^2/2$. Tumour volumes were measured by an investigator blinded to group allocation. At the study endpoint, mice were deeply anesthetized with sodium pentobarbital (50 mg/kg, intraperitoneal injection of a 2.5 solution) and euthanized by cervical dislocation after loss of consciousness was confirmed. Death was confirmed by cessation of respiration and heartbeat before tumor harvest. Tumors were excised, weighed, and processed for downstream analysis. The primary outcome measure was tumor growth inhibition, assessed by tumor volume. Tumor volume was measured every 3 days and final tumor volume was measured at the study endpoint. Secondary outcome measures included the proportions of MDSCs, CD4+ T cells, CD8+ T cells, PD1+CD8+ T cells, and IFN-γ+CD8+ T cells in tumor tissues. All endpoint analyses were performed after two weeks of treatment. The study was conducted in compliance with the guidelines of the Institutional Animal Care and Use Committee of Shanghai General Hospital (2025AWS615).

2.6 Flow Cytometry

To facilitate analyses of immune cell populations, tumor tissues were dissociated into single-cell suspensions for flow cytometry [37]. Flow cytometry was conducted by an operator blinded to group assignment throughout data acquisition and analysis. Cells were stained with a panel of antibodies specific for APC-A750 live/dead stain (L/D) to exclude dead cells, PB450 anti-CD45 (BioLegend, 103125), PE anti-Ly6g (BD Biosciences, 551461), PC7 anti-Ly6c (Thermo Fisher Scientific, 25-5932-82), and APC anti-CD11b (BioLegend, 101211); And APC-Cy7 live/dead stain (L/D), PerCP-Cy5.5 anti-CD45 (BioLegend, 103131), BB515 anti-CD8 (BD Biosciences, 564422), BV605 anti-CD4 (BD Biosciences, 563151), PE anti-PD1 (BioLegend, 109103), and BV650 (anti-Interferon-γ) anti-IFN-γ (BioLegend, 505831). Surface staining was performed for 30 min at 4 °C in the dark. For intracellular IFN-γ staining, cells were stimulated with PMA and ionomycin in the presence of a protein transport inhibitor for 4–6 h, followed by fixation/permeabilization according to the manufacturer's instructions and intracellular staining with anti-IFN-γ antibody. A BD LSRFortessa flow cytometer was used to acquire all data using the BD FACSDiva software, followed by analysis with FlowJo (v7.5.5, FlowJo, LLC, Ashland, Oregon, USA).

2.7 Statistical Analysis

Statistical analyses were performed using GraphPad Prism software version 9.5.1 (GraphPad Software, San Diego, CA, USA). For in vivo experiments, the individual mouse was considered the experimental and statistical unit. Normality was assessed using the Shapiro-Wilk test, and homogeneity of variance was assessed using Brown-Forsythe or Levene's test where appropriate. For comparisons between two groups, Student's *t*-test was used for normally distributed data with equal variance, while the Wilcoxon rank-sum test was used for non-normally distributed data. For comparisons among multiple groups, one-way ANOVA followed by appropriate multiple-comparison testing was used for endpoint measurements, and two-way ANOVA was used for tumor growth curves over time. Kaplan-Meier survival analysis was performed using the log-rank test. Data are presented as mean $\pm$ SD or mean $\pm$ SEM as indicated in the figure legends. Exact p values were reported where appropriate, and $p < 0.05$ was considered statistically significant.

3. Results

3.1 Elevated DKK1 Expression is Associated With Poor HNSCC Patient Prognosis

To explore the prognostic significance of DKK1 expression in HNSCC, we initially analyzed data from TCGA database. A scatter plot highlighting the association between DKK1 expression levels and HNSCC patients OS revealed a positive correlation between higher DKK1 ex-

pression and increased mortality (Fig. 1a). Kaplan-Meier survival analysis further confirmed that patients with high DKK1 expression (n = 251) exhibit significantly shorter OS compared to those with low DKK1 expression (n = 252), with a hazard ratio (HR) of 2.07 (95% CI: 1.57–2.73, $p < 0.001$) (Fig. 1b). Significantly higher DKK1 expression was also observed in tumor tissues compared to normal tissues ($p < 0.001$) (Fig. 1c), indicating a potential role for DKK1 in tumor progression. To examine the association between DKK1 expression and tumor stage, we further analyzed DKK1 levels in different pathological T stages within the TCGA dataset. As shown in **Supplementary Fig. 1**, DKK1 expression was significantly higher in advanced-stage tumors (T3,T4) as compared to early-stage tumors (T1, T2) ($p < 0.01$), suggesting that elevated DKK1 levels may correlate with tumor progression. To further validate these findings, we analyzed clinical samples from 62 HNSCC patients at Shanghai General Hospital. The patients were categorized into DKK1-high and DKK1-low groups based on IHC staining results for DKK1. As expected, the DKK1-high group exhibited markedly stronger DKK1 staining intensity in tumor tissues (Fig. 1d). Kaplan-Meier analysis of this cohort showed that elevated DKK1 expression was significantly associated with a worse prognosis (Fig. 1e), highlighting its correlation with reduced survival outcomes. These results align with the findings from the TCGA dataset, underscoring the role of DKK1 as an adverse prognostic factor in HNSCC.

3.2 DKK1 Expression Correlates With Immunosuppressive Features in the HNSCC Immune Microenvironment

To explore the connection between DKK1 expression and the immune microenvironment in HNSCC, single-cell RNA sequencing (scRNA-seq) analysis was conducted using the GSE103322 dataset. The t-SNE plot shown in Fig. 2a was used for cell clustering, identifying distinct immune cell populations, including CD4+ T cells, CD8+ T cells, myeloid cells, endothelial cells, and tumor cells. When DKK1 expression was examined across cell types (Fig. 2b), it was found to be predominantly expressed in tumor cells, with minimal expression in other cell types.

To further explore how DKK1 expression affects immune cell infiltration within tumors, we stratified the TCGA HNSCC samples into DKK1-high and DKK1-low groups based on expression data and analyzed the immune cell composition in each group. As shown in the stacked bar plot in Fig. 2c, the DKK1-high group exhibited a lower proportion of CD8+ T cells and an increased presence of immunosuppressive cell types compared to the DKK1-low group. A heatmap was generated to illustrate the abundance of different immune cell types in these DKK1 expression-based groups (**Supplementary Fig. 2a**), revealing significant differences in the abundance of CD8+ T cells, CD4+ T cells, and B cells. Correlation heatmap analysis further highlighted a significant negative correlation between DKK1 expression and CD8+ T cells, whereas DKK1 levels were positively correlated with the abundance of immunosuppressive cells, such as monocytes and neutrophils (Fig. 2d, **Supplementary Fig. 2b**). Spearman correlation analysis additionally revealed a negative correlation between the expression of DKK1 and the T cell, CD8+T cell and cytotoxic T cell scores (Fig. 2e, **Supplementary Fig. 2c**), further suggesting that high levels of DKK1 expression may promote an immunosuppressive TME in HNSCC.

3.3 Clinical Validation of DKK1 Expression and Its Impact on the Immune Microenvironment in HNSCC

To further confirm the association between DKK1 expression and immune cell infiltration in HNSCC, we analyzed tumor samples from the 62 patients in the Shanghai General Hospital cohort detailed above. IHC and immunofluorescence staining were performed to detect CD8, PDL1, CD15, and CD14 expression in tumor tissues with low and high DKK1 expression (Fig. 3a). Representative images illustrate that tumors with high levels of DKK1 expression displayed significantly reduced CD8+ T cells infiltration, together with an increased in the presence of PDL1+ and CD15+ cells, as compared to tumors exhibiting low levels of DKK1 expression. Quantification of immune cell markers confirmed that tumors with high DKK1 expression harbor significantly fewer CD8+ T cells ($p < 0.0001$) and higher numbers of PDL1+ ($p < 0.0001$) and CD15+ cells ($p < 0.0001$) per FOV (Fig. 3b). However, as shown in **Supplementary Fig. 3**, no significant difference in CD14+ cells infiltration was observed between the DKK1 high and low expression groups. These findings suggest that high DKK1 expression in HNSCC is associated with an immunosuppressive microenvironment characterized by decreased cytotoxic T cells infiltration and increased expression of immunosuppressive markers.

3.4 Construction and Analysis of HNSCC Patient-Derived Tumor Immune Organoids

To investigate the effects of anti-DKK1 treatment on the TME, we constructed HNSCC patient-derived tumor immune organoids, incorporating both tumor cells and immune cells to mimic the native tumor-immune interactions. The schematic in Fig. 4a illustrates the process used to prepare these 3D organoid models, which closely mirror the architecture and cellular composition of HNSCC tumors.

Representative images of tumor immune organoids cultured under standard conditions are shown in Fig. 4b. Following treatment with anti-DKK1, the tumor organoids exhibited a noticeable reduction in size compared to the control group, suggesting that anti-DKK1 effectively suppresses tumor growth within the tumor-immune microenvironment. Quantification of tumor organoid size further confirmed the inhibitory effect of anti-DKK1 treatment (Fig. 4c), with a significant reduction in organoid number compared to the control group.

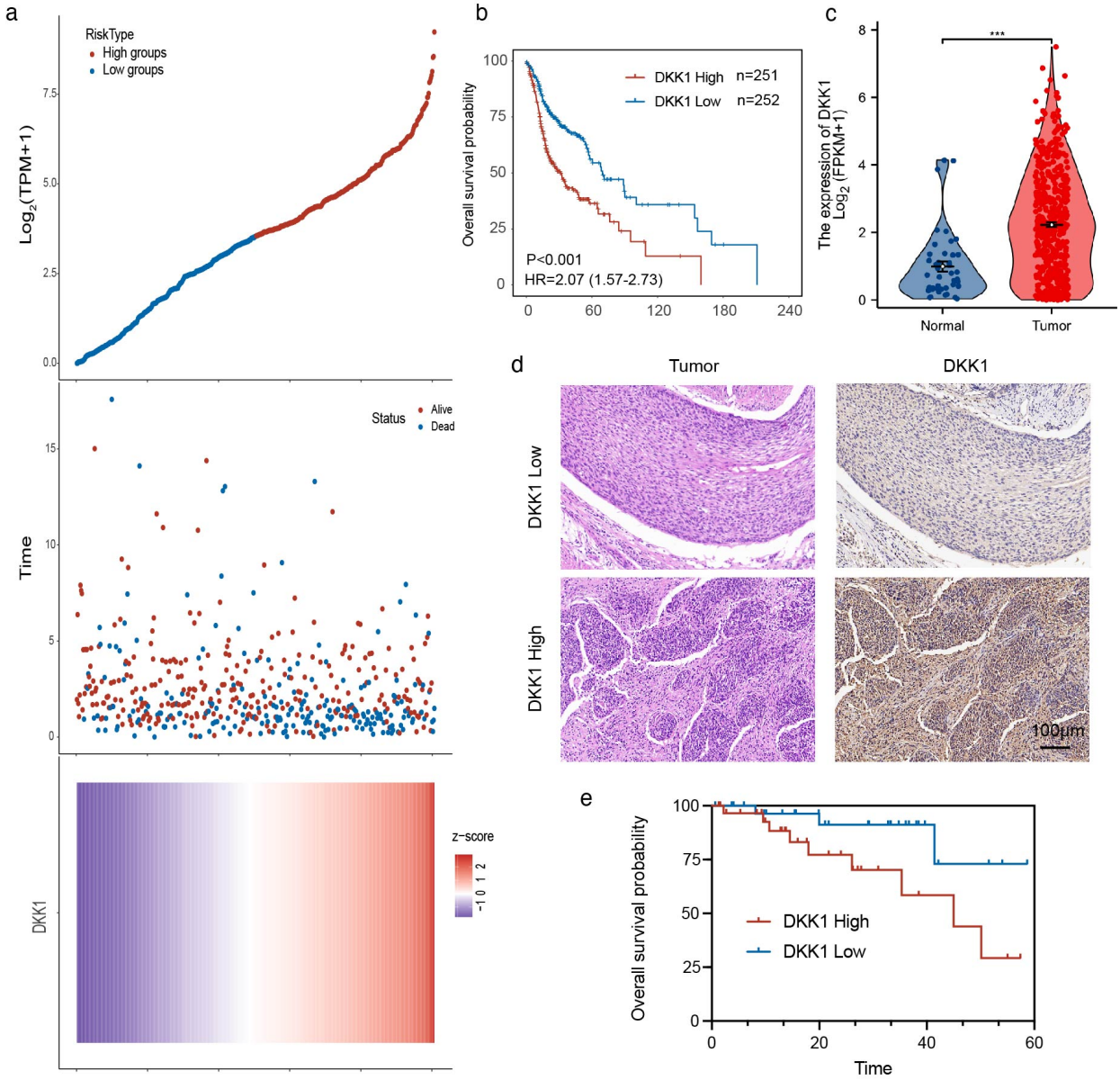

Fig. 1. Elevated DKK1 expression correlates with poor prognosis in head and neck squamous cell carcinoma (HNSCC). (a) Analysis of DKK1 expression in HNSCC patients from the TCGA database. The upper panel shows a scatter plot of DKK1 expression (Log_2(TPM+1)) ranked from low to high expression, color-coded by risk type (high vs. low groups). The middle panel displays a scatter plot of survival time and status, with red representing deceased patients and blue representing surviving patients. The lower panel is a heatmap showing DKK1 expression levels (z-score) across patient samples. (b) Kaplan-Meier survival analysis based on DKK1 expression in HNSCC patients from the TCGA dataset. Patients with high DKK1 expression (n = 251) show significantly worse overall survival compared to those with low DKK1 expression (n = 252), with a hazard ratio (HR) of 2.07 (95% CI: 1.57–2.73) and $p <$ 0.001. Statistical analysis was performed using the Kaplan-Meier method with log-rank test. (c) Comparison of DKK1 expression levels (Log_2(FPKM+1)) between normal and tumor tissues in HNSCC patients, indicating significantly elevated expression in tumor tissues (***$p < 0.001$). Statistical significance was evaluated using the Wilcoxon rank-sum test. (d) Representative H&E and immunohistochemistry (IHC) staining images for DKK1 in tumor tissues from clinical HNSCC samples (Shanghai General Hospital cohort), showing the DKK1-low and DKK1-high groups. Scale bar, 100 μm. (e) Kaplan-Meier survival curve for overall survival in the Shanghai General Hospital cohort (n = 62), comparing patients with high and low levels of DKK1 expression, revealing that high DKK1 expression is associated with significantly worse prognosis. Statistical significance was evaluated using the log-rank test. DKK1, Dickkopf-Related Protein 1; TCGA, The Cancer Genome Atlas.

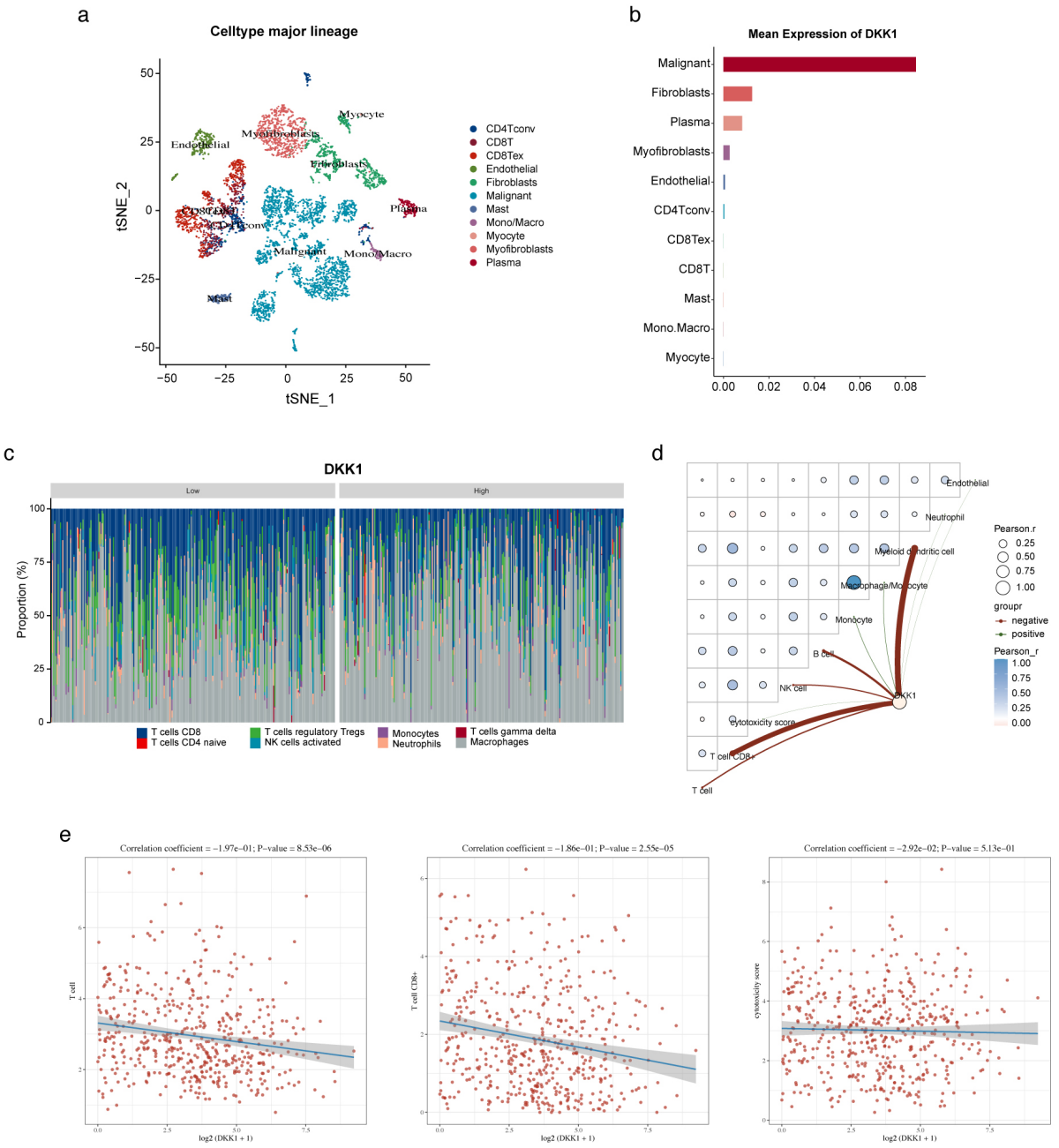

Fig. 2. Association between DKK1 expression and the composition of the immune microenvironment in HNSCC. (a) t-SNE plot showing cell clusters generated based on single-cell RNA sequencing data from the GSE103322 HNSCC dataset. Each color represents a distinct cell type, including CD4+ T cells, CD8+ T cells, endothelial cells, malignant cells, and various immune cell subsets. (b) Bar plot of DKK1 expression levels across different cell types in HNSCC (GSE103322). (c) Stacked bar plot displaying the proportions of various immune cell types between the groups exhibiting high and low DKK1 expression based on TCGA data. (d) Correlation heatmap illustrating the relationship between immune scores and gene expression profiles in HNSCC. Red and green respectively denote positive and negative correlations. Circle size is proportional to correlation strength, with larger circles indicating stronger correlations. Red and green lines respectively represent negative and positive correlations between immune scores or gene expression and DKK1 expression. (e) Spearman correlation analysis of the association between DKK1 expression and immune scores in HNSCC. Each scatter plot represents the correlation between DKK1 expression and different immune cell scores, with each point representing an individual sample. X-axis denotes DKK1 expression, and Y-axis denotes immune scores. A positive correlation coefficient indicates a direct relationship, while a negative correlation coefficient indicates an inverse relationship. Statistical analysis was performed using Spearman correlation analysis.

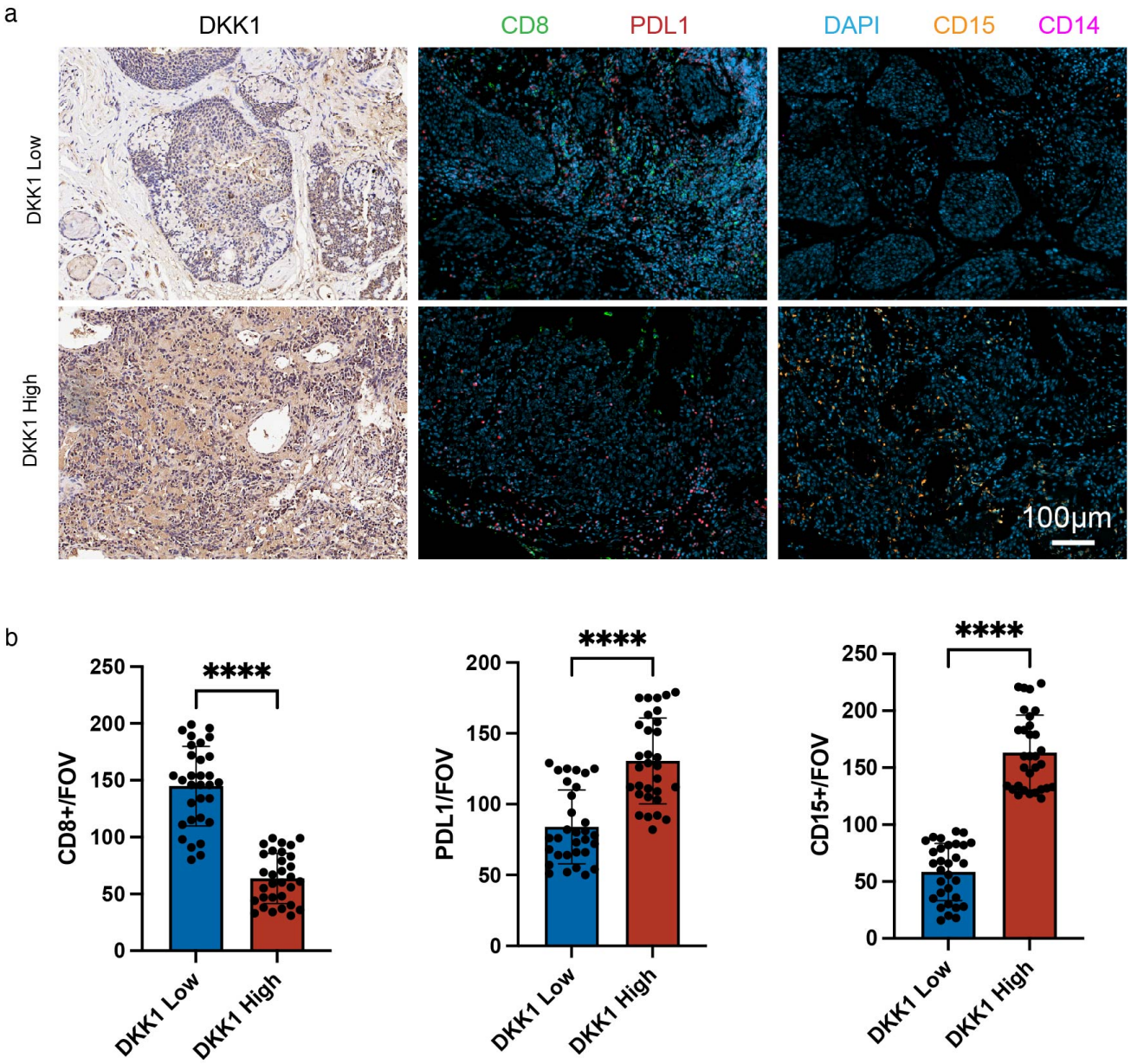

Fig. 3. Clinical validation of DKK1 expression and its association with the composition of the immune microenvironment in HNSCC patients. (a) Immunohistochemistry (IHC) and immunofluorescence staining for DKK1, CD8, PDL1, CD15, and CD14 in tumor samples from HNSCC patients with low and high levels of DKK1 expression (n = 62). Representative images show differences in immune cell infiltration between the DKK1-low and DKK1-high groups. Left panel: IHC staining for DKK1; middle panel: immunofluorescence staining for CD8 (green) and PDL1 (red); right panel: immunofluorescence staining for CD15 (orange) and CD14 (purple) with DAPI nuclear staining (blue). Scale bar, 100 μm. (b) Quantification of CD8+, PDL1+, and CD15+ cells per field of view (FOV) in DKK1-low and DKK1-high groups. Data represent the mean ± SD, n = 62 HNSCC patients from Shanghai General Hospital (n = 62). ****$p < 0.0001$.

3.5 Combined Anti-DKK1 and Anti-PD1 Therapy Enhances Anti-PD1 Efficacy

Given the association between DKK1 and immunosuppressive features in HNSCC, we hypothesized that targeting DKK1 may augment the efficacy of anti-PD1 immunotherapy. To test this possibility, we utilized the TCGA dataset to analyze the expression of various immune checkpoint genes in DKK1-high and DKK1-low patient groups. As shown in Fig. 5a, immune checkpoint genes including *PDCD1* (encoding PD-1), *LAG3*, and *TIGIT* were significantly upregulated in the DKK1-high group, indicating that patients with elevated levels of DKK1 expression may exhibit an immunosuppressive intratumoral phenotype that may constrain the efficacy of anti-PD1 treatment. This

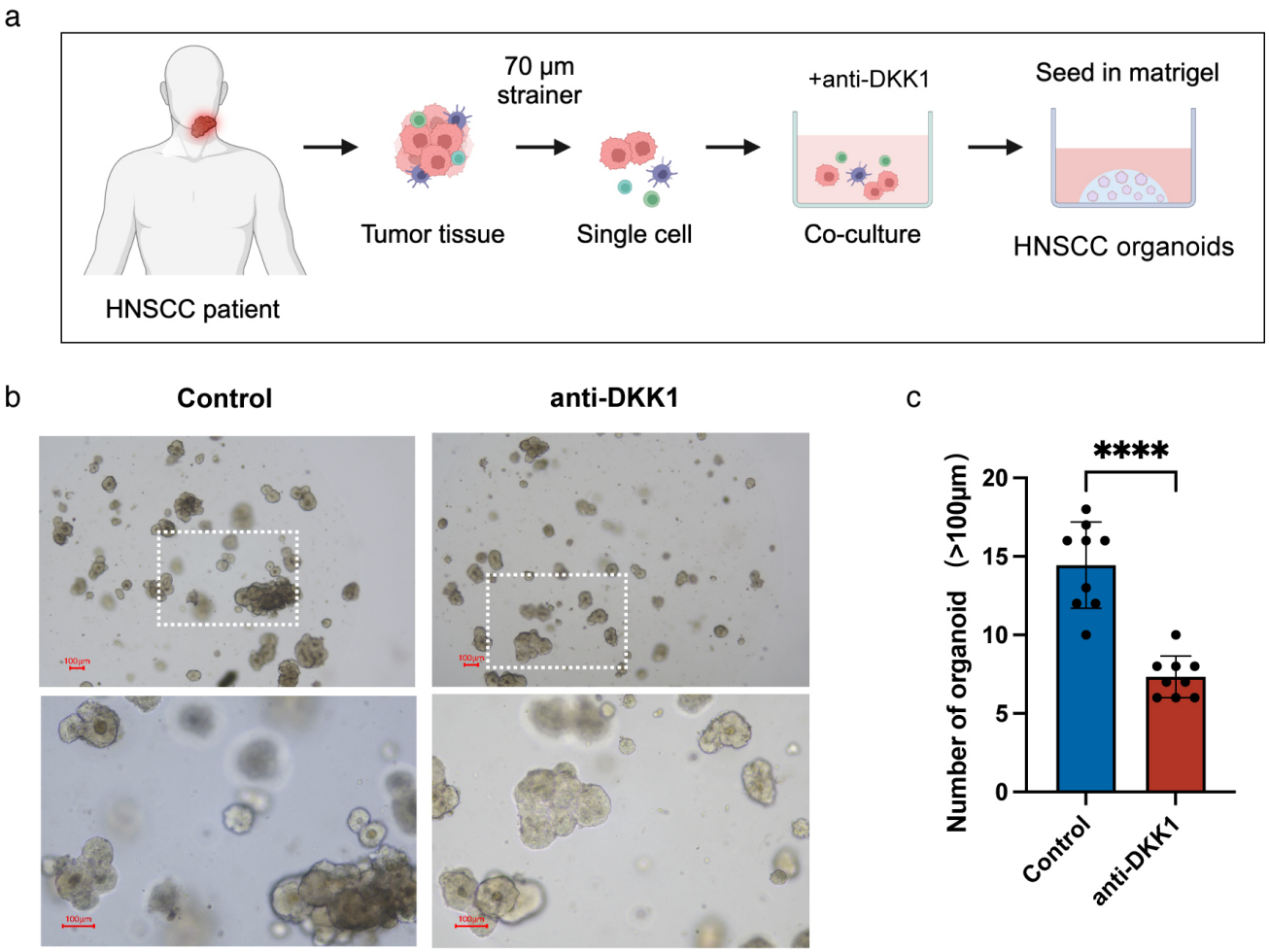

Fig. 4. Construction and analysis of HNSCC patient-derived tumor immune organoids. (a) Schematic illustration of the process for constructing HNSCC patient-derived tumor immune organoids. Created in BioRender. Yin, Y. (2026) https://BioRender.com/fza4mOk. (b) Representative images of HNSCC patient-derived tumor organoids cultured under standard conditions following anti-DKK1 treatment. Scale bars represent 100 µm. (c) Quantification of tumor Number of large organoids following anti-DKK1 treatment, showing a significant reduction in size compared to the control group. Organoids were derived from 10 independent HNSCC patients. Statistical significance was evaluated using Student's *t*-test or Wilcoxon rank-sum test. ****$p < 0.0001$.

increased immune checkpoints molecule expression in the DKK1-high group suggests that these tumors may rely on multiple inhibitory pathways to evade immune detection, further supporting the need to employ a combined targeting approach.

To further assess the potential benefit of DKK1 inhibition, we utilized the Tumor Immune Dysfunction and Exclusion (TIDE) algorithm to predict tumor responsiveness to immune checkpoint inhibitor (ICI) treatment. As shown in Fig. 5b, the TIDE score of DKK1-low patients was significantly lower than that of DKK1-high patients, suggesting that these HNSCC patients may respond more strongly to ICIs as compared to those with high levels of DKK1 expression ($p < 0.01$).

We then evaluated the therapeutic effects of anti-DKK1 and anti-PD1 combination therapy in a subcutaneous mouse model of HNSCC. Tumor images (Fig. 5c) and growth curves (Fig. 5d) revealed that combination therapy significantly reduced tumor size compared to control tumor growth or monotherapy treatment with anti-PD1, or anti-DKK1. Final tumor weights (Fig. 5e) also indicated a substantial reduction in the combination therapy group ($p < 0.0001$), highlighting the enhanced efficacy of anti-DKK1 and anti-PD1 co-administration.

3.6 Anti-DKK1 and Anti-PD1 Combination Therapy Modulates the Tumor Immune Microenvironment

To understand how anti-DKK1 and anti-PD1 combination therapy influences the tumor immune microenvironment, we conducted a flow cytometry-based analysis of tumor-infiltrating immune cells in our experimental mouse model system. Representative gating strategies for the identification of MDSCs and T-cell subsets are shown in **Supplementary Fig. 4**. As shown in Fig. 6a, staining for Ly6g

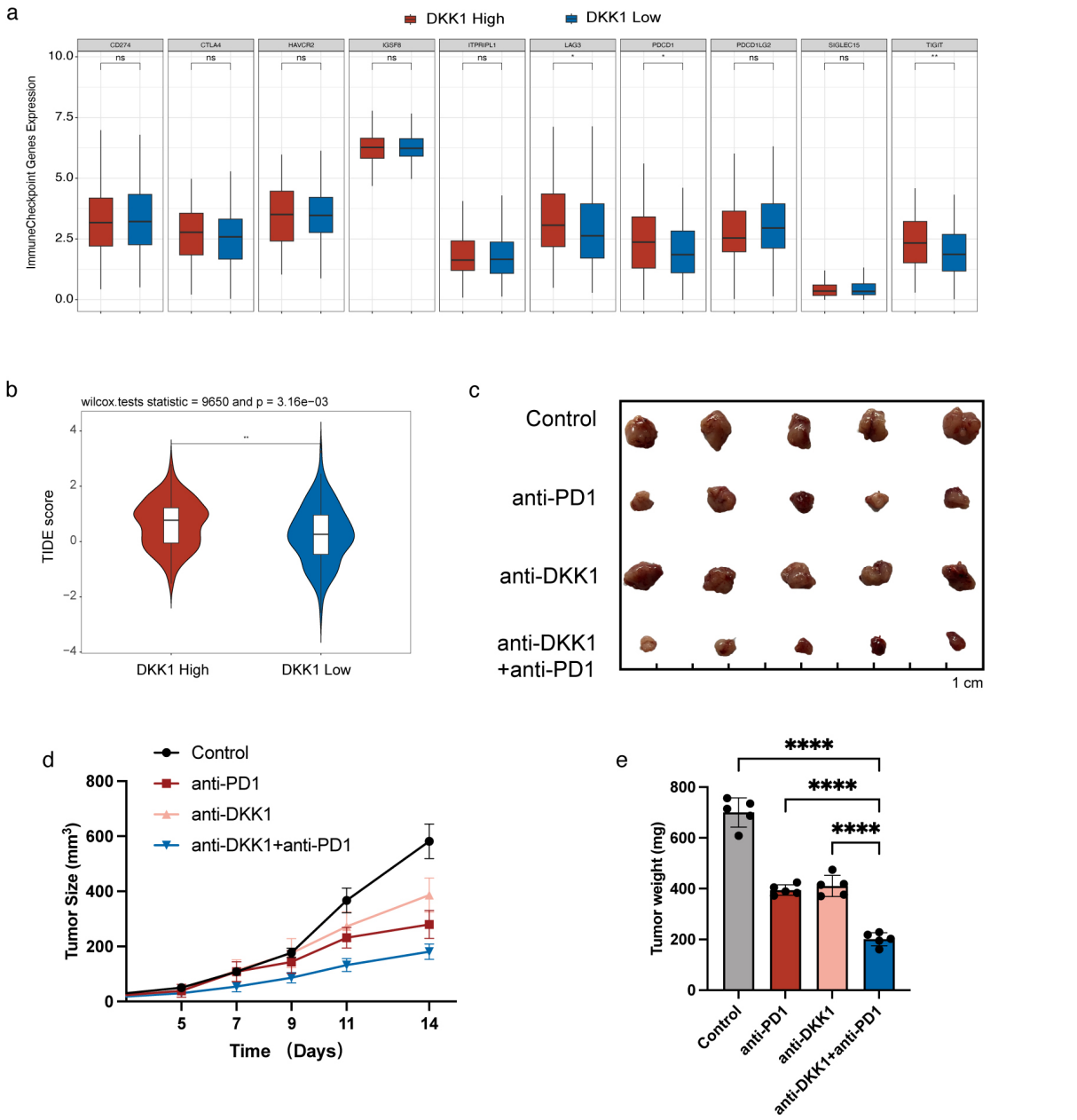

Fig. 5. Anti-DKK1 therapy enhances the efficacy of anti-PD1 treatment in HNSCC. (a) Immune checkpoint gene expression profiles for tumors in the DKK1-high and DKK1-low groups in the TCGA dataset. The x-axis represents different immune checkpoint genes, while the y-axis represents expression levels. Box plots compare gene expression between DKK1 high (red) and low (blue) groups. Statistical significance is indicated by asterisks (*$p < 0.05$, **$p < 0.01$, ns $p > 0.05$), evaluated using the Wilcoxon rank-sum test. (b) Predicted immune response scores in the DKK1-high and DKK1-low groups based on the Tumor Immune Dysfunction and Exclusion (TIDE) algorithm. The violin plot shows the distribution of TIDE scores, indicating that the DKK1 low group has a higher predicted response to immune checkpoint inhibitors. Statistical significance was assessed by Wilcoxon test, with **$p < 0.01$. (c) Representative images of tumors in a subcutaneous mouse tumor model treated with control, anti-PD1, anti-DKK1, or a combination of anti-DKK1 and anti-PD1. Scale bar, 1 cm. (d) Tumor growth curves for the indicated treatment groups, showing that the combination of anti-DKK1 and anti-PD1 significantly suppresses tumor growth compared to individual treatments (n = 5 mice per group). Data are shown as mean ± SD. (e) Final tumor weights in each treatment group, demonstrating the enhanced antitumor effect of combined anti-DKK1 and anti-PD1 therapy. ****$p < 0.0001$, indicating a highly significant reduction in tumor weight with combination therapy. Statistical significance was evaluated using Student's *t*-test or Wilcoxon rank-sum test, as appropriate. PD-1, Programmed Cell Death Protein 1.

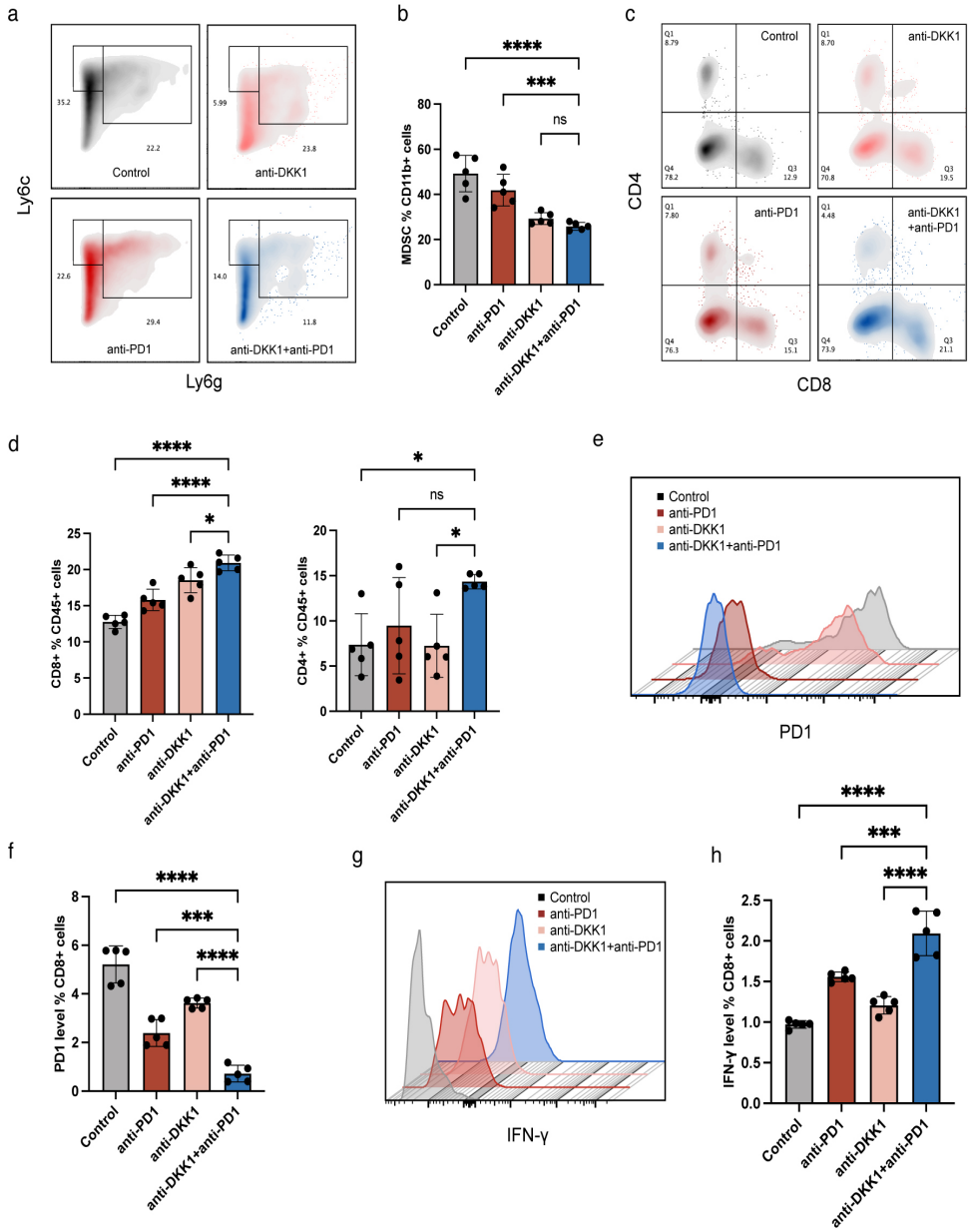

Fig. 6. Modulation of the tumor immune microenvironment by combined anti-DKK1 and anti-PD1 therapy. (a) Flow cytometry plots showing Ly6g and Ly6c staining of CD11b+ cells across treatment groups (Control, anti-PD1, anti-DKK1, and anti-DKK1 + anti-PD1; n = 5 mice per group). (b) Quantification of MDSC (CD11b+Ly6g+Ly6c+) populations in each treatment group, indicating a significant reduction in MDSCs with anti-PD1 and anti-DKK1 combination therapy. $^{****}p < 0.0001$, $^{***}p < 0.001$; ns: not significant. (c) Flow cytometry plots of CD4+ and CD8+ T cell populations in each treatment group, highlighting the impact of combined therapy on T cell composition. (d) Quantification of CD8+ and CD4+ T cells (as percentages of CD45+ cells) in each treatment group. Anti-DKK1 + anti-PD1 combination therapy significantly increases the proportion of CD8+ T cells, while CD4+ T cell levels show minor variations. Student's *t*-test or Wilcoxon rank-sum test, as appropriate. $^{*}p < 0.05$, $^{****}p < 0.0001$, ns $p > 0.05$. (e) Flow cytometry histograms showing PD1 expression in CD8+ T cells across treatment groups, with a marked reduction in the anti-DKK1 + anti-PD1 group. (f) Quantification of PD1+ CD8+ T cells, with significantly lower PD1 levels in the anti-DKK1 + anti-PD1 group, indicating enhanced T cell activation. Statistical significance was evaluated using Student's *t*-test or Wilcoxon rank-sum test, as appropriate. $^{****}p < 0.0001$, $^{***}p < 0.001$. (g) Flow cytometry histograms showing IFN-γ expression in CD8+ T cells across treatment groups, with a notable increase in the anti-DKK1 + anti-PD1 group. (h) Quantification of IFN-γ+ CD8+ T cells, demonstrating a significant increase in IFN-γ production with combination therapy, indicative of heightened T cell activity. $^{****}p < 0.0001$, $^{***}p < 0.001$. Statistical significance was evaluated using Student's *t*-test or Wilcoxon rank-sum test, as appropriate. MDSC, Myeloid-Derived Suppressor Cells; IFN-γ, Interferon-γ.

and Ly6c expression among CD11b+ cells revealed a significant reduction in MDSCs abundance in the combination therapy group compared to the control and monotherapy groups. Quantification of MDSC proportions (Fig. 6b) further confirmed that the combination therapy group had the lowest MDSC levels among all treatment groups ($p < 0.0001$), indicating a reduction in immunosuppression.

Additionally, we assessed CD4+ and CD8+ T cell infiltration (Fig. 6c,d). Combination therapy administration significantly increased the proportion of CD8+ T cells within the TME compared to the other groups ($p < 0.05$), consistent with the enhancement of cytotoxic T cell infiltration. With respect to CD4+ T cells, we found that the combination therapy group exhibited a higher number of CD4+ T cells than the control and anti-DKK1 groups ($p < 0.05$), although the difference was not statistically significant compared to the anti-PD1 monotherapy group. Further analysis of PD1 expression on CD8+ T cells showed that combination therapy markedly decreased PD1 expression (Fig. 6e,f), suggesting a reduction in T cell exhaustion. To evaluate T cell functional activation, we examined IFN-γ production by CD8+ T cells. Flow cytometry histograms (Fig. 6g) and quantification (Fig. 6h) revealed significantly higher IFN-γ levels in the combination therapy group ($p < 0.0001$), consistent with enhanced cytotoxic T cell activity. These findings collectively suggest that anti-DKK1 and anti-PD1 combination therapy promotes an immunostimulatory microenvironment within HNSCC tumors characterized by reduced immunosuppression, increased CD8+ T cell infiltration, and heightened T cell activation.

4. Discussion

This study offers new insight into the role of DKK1 as a key regulator of the immune microenvironment in HNSCC. We found that elevated DKK1 expression is associated with poor prognosis in HNSCC, potentially owing to its ability to foster an immunosuppressive TME. Our results also highlight the potential of targeting DKK1 in combination with ICIs, as co-administration of anti-DKK1 and anti-PD1 led to enhanced antitumor immunity and reduced tumor growth in preclinical models of HNSCC.

The immunosuppressive effects of DKK1 appear to be mediated, in part, by its influence on immune cell composition within the TME. Elevated DKK1 expression was linked to decreased infiltration of cytotoxic CD8+ T cells, which are crucial for effective antitumor immunity and responsiveness to ICIs [38]. Additionally, our data revealed that DKK1 promotes an immunosuppressive environment by facilitating the accumulation of MDSCs, which are known to inhibit T cell activation and expansion [39], further dampening the antitumor immune response. This pattern of immune cell distribution likely explains the poor response to immunotherapy observed in patients with elevated DKK1 levels. A possible molecular explanation for this effect is that DKK1 may directly regulate MDSC biology through suppression of β-catenin signaling. Previous studies have shown that downregulation of β-catenin in MDSCs is critical for their accumulation and suppressive activity [17], and that DKK1 can directly target these cells to inhibit β-catenin signaling, thereby promoting both MDSC expansion and immune suppressive function. In contrast, DKK1 neutralization was reported to rescue β-catenin signaling in MDSCs, reduce their accumulation, and restore T-cell recruitment at tumor sites. Therefore, our findings raise the possibility that elevated DKK1 in HNSCC may contribute to an immunosuppressive microenvironment, at least in part, by enhancing MDSC-mediated immune suppression through a β-catenin-dependent mechanism.

The inverse relationship that we identified between DKK1 expression and CD8+ T cell infiltration is particularly relevant for efforts aimed at improving immunotherapy outcomes. ICIs, such as anti-PD1 therapy, rely on an active and T cell-enriched immune environment to be effective. In our study, we observed a less pronounced T-cell-inflamed signature in the DKK1-high group, suggesting a less favorable environment for ICI efficacy. By inhibiting DKK1, we were able to counteract this immunosuppressive environment, as evidenced by an increase in CD8+ T cell infiltration and activation when anti-DKK1 was combined with anti-PD1 therapy. This combination enhanced the recruitment of cytotoxic T cells while also increasing their functional activation, as indicated by higher levels of IFN-γ production. In addition, the TIDE analysis in our study suggested that tumors with low DKK1 expression may be more likely to respond to immune checkpoint blockade. However, this result should be interpreted cautiously, as TIDE is a computational prediction tool and does not constitute direct experimental or clinical validation of immunotherapy response.

The use of tumor immune organoids, as employed in our study, provides a powerful *in vitro* model capable of simulating the tumor-immune microenvironment and testing the effects of DKK1 inhibition in a clinically relevant context. Tumor immune organoids derived from HNSCC patient samples were constructed through the co-culture of tumor cells with TME-derived immune cells, thereby closely mimicking the complex cellular interactions and immune dynamics of the patient's TME. This innovative approach allows for the more accurate recapitulation of immune cell infiltration and tumor growth observed *in vivo*, enabling the precise evaluation of combination therapies, including anti-DKK1 and ICIs, in a controlled setting. These models also serve as a versatile platform for screening other potential immune-modulating compounds. For example, natural agents such as trans-resveratrol and rhodioloside have shown promising immunomodulatory and anti-tumor effects [40]. Their combination with DKK1-targeted and ICIs therapies could further amplify anti-tumor immune responses and improve treatment outcomes. This

ability to establish patient-relevant models underscores the potential of tumor immune organoids in advancing personalized cancer therapy and understanding immune interactions within the TME.

Our findings suggest that DKK1 may serve as a valuable therapeutic target in HNSCC, particularly for patients who may not respond adequately to anti-PD1 monotherapy. The use of anti-DKK1 therapy to reduce MDSC levels and boost CD8+ T cell activity within the TME could enhance the overall efficacy of immunotherapy. This approach aligns with the growing emphasis on targeting specific elements of the TME to overcome resistance mechanisms and improve outcomes in immunotherapy-resistant cancers. The relationship between DKK1 and the immune microenvironment also highlights the broader role of DKK1 as a context-dependent modulator in cancer biology. In this study, DKK1 appears to act as an oncogenic factor, promoting an immune-suppressive TME that favors tumor growth and immune evasion. Unlike conventional biomarkers, which often reflect only a single aspect of tumor biology, DKK1 demonstrates a multifaceted influence, affecting both the recruitment and functional activity of immune cells. Further investigation of these effects may help inform the development of DKK1-targeted therapies for HNSCC immunotherapy.

In conclusion, our findings support a role for DKK1 in immune suppression in HNSCC and suggest that it may represent a potential target for combination immunotherapy. By alleviating DKK1-mediated immunosuppression, combination therapy with anti-DKK1 and anti-PD1 therapy may offer promise as a means of enhancing antitumor immunity in HNSCC. Future studies will be needed to validate these findings in clinical settings and to optimize DKK1-targeted therapies for integration with current immunotherapy protocols. Overall, our results provide a preclinical rationale for further investigation of DKK1-targeted combination therapy in HNSCC.

5. Limitations

This study has several limitations. Although we integrated TCGA analysis, a clinical cohort, patient-derived tumor immune organoids, and an *in vivo* murine model, the clinical cohort was relatively small and derived from a single center, which may limit the generalizability of the findings. In addition, while our data support an association between elevated DKK1 expression and an immunosuppressive tumor microenvironment, the precise molecular mechanisms by which DKK1 regulates immune cell function were not directly dissected in this study. Moreover, although the tumor immune organoid model represents a major strength of this work, it cannot fully recapitulate the complexity of the *in vivo* tumor microenvironment. However, these limitations do not affect the main conclusion that DKK1 is associated with an immunosuppressive microenvironment in HNSCC and may represent a potential target for combination immunotherapy. Future studies with larger multicenter cohorts and more detailed mechanistic investigations will be needed to further validate and extend these observations.

6. Conclusions

This study highlights the critical role of DKK1 as a driver of immune suppression in the TME of HNSCC. High DKK1 expression is correlated with poor patient outcomes and gives rise to localized immunosuppressive conditions within tumors by reducing CD8+ T cell infiltration and enhancing MDSCs abundance. By targeting DKK1, we were able to significantly enhance antitumor immunity in preclinical models, particularly when combined with anti-PD1 therapy, which resulted in reduced tumor growth, increased CD8+ T cell activity, and a more immunostimulatory TME in both *in vivo* models and patient-derived tumor immune organoids. The approach used to grow and utilize tumor immune organoids in this study also offers an innovative approach for modeling the TME, enabling precise evaluation of therapeutic strategies. These findings underscore the therapeutic potential of DKK1 inhibition as a complement to the use of immune checkpoint inhibitors, offering a promising avenue for improving immunotherapy outcomes in HNSCC. Future research should focus on translating these findings to clinical settings and exploring DKK1-targeted combination therapies in broader patient populations.

Abbreviations

HNSCC, Head and Neck Squamous Cell Carcinoma; DKK1, Dickkopf-Related Protein 1; TME, Tumor Microenvironment; ICIs, Immune Checkpoint Inhibitors; PD-1, Programmed Cell Death Protein 1; PD-L1, Programmed Cell Death Ligand 1; MDSCs, Myeloid-Derived Suppressor Cells; CD8+ T cells, Cluster of Differentiation 8 Positive T Cells; IHC, Immunohistochemistry; scRNA-seq, Single-Cell RNA Sequencing; TCGA, The Cancer Genome Atlas; OS, Overall Survival; FOV, Field of View; IL-2, Interleukin-2; MACS, Magnetic-Activated Cell Sorting.

Availability of Data and Materials

The datasets analyzed during the current study are available from The Cancer Genome Atlas (TCGA) repository and the GSE103322 dataset. Additional data generated and analyzed during this study are available from the corresponding author upon reasonable request.

Author Contributions

FW designed the study, conducted data analysis, and wrote the manuscript. XD, MY and ZZ performed the animal and organoid experiments and contributed to data acquisition. PD and XC supervised the study, interpreted the findings, and reviewed the manuscript. All authors read and

approved the final manuscript. All authors contributed to editorial changes in the manuscript. All authors have participated sufficiently in the work and agreed to be accountable for all aspects of the work.

Ethics Approval and Consent to Participate

This study was conducted in accordance with the ethical principles of the Declaration of Helsinki and approved by the Institutional Review Board of Shanghai General Hospital (2020KY144). All participants provided written informed consent before sample collection and data analysis. The animal study was conducted in compliance with the guidelines of the Institutional Animal Care and Use Committee of Shanghai General Hospital (approval number: 2025AWS615). All procedures strictly followed the 3Rs principle (Replacement, Reduction, and Refinement). This study was carried out in compliance with the ARRIVE guidelines.

Acknowledgment

The authors thank the staff of Shanghai General Hospital for their assistance in clinical data collection and all study participants for their valuable contributions.

Funding

This work was supported by grants from The National Natural Science Foundation of China (Grant No 82072989).

Conflicts of Interest

The authors declare no conflicts of interest.

Supplementary Material

Supplementary material associated with this article can be found, in the online version, at https://doi.org/10.31083/FBL50766.

References

[1] Johnson DE, Burtness B, Leemans CR, Lui VWY, Bauman JE, Grandis JR. Head and neck squamous cell carcinoma. Nature Reviews. Disease Primers. 2020; 6: 92. https://doi.org/10.1038/s41572-020-00224-3.

[2] Thawani R, Kim MS, Arastu A, Feng Z, West MT, Taflin NF, *et al*. The contemporary management of cancers of the sinonasal tract in adults. CA: a Cancer Journal for Clinicians. 2023; 73: 72–112. https://doi.org/10.3322/caac.21752.

[3] Mody MD, Rocco JW, Yom SS, Haddad RI, Saba NF. Head and neck cancer. Lancet (London, England). 2021; 398: 2289–2299. https://doi.org/10.1016/S0140-6736(21)01550-6.

[4] Bhatia A, Burtness B. Treating Head and Neck Cancer in the Age of Immunotherapy: A 2023 Update. Drugs. 2023; 83: 217–248. https://doi.org/10.1007/s40265-023-01835-2.

[5] Sun JM, Shen L, Shah MA, Enzinger P, Adenis A, Doi T, *et al*. Pembrolizumab plus chemotherapy versus chemotherapy alone for first-line treatment of advanced oesophageal cancer (KEYNOTE-590): a randomised, placebo-controlled, phase 3 study. Lancet (London, England). 2021; 398: 759–771. https://doi.org/10.1016/S0140-6736(21)01234-4.

[6] Mei Z, Huang J, Qiao B, Lam AKY. Immune checkpoint pathways in immunotherapy for head and neck squamous cell carcinoma. International Journal of Oral Science. 2020; 12: 16. https://doi.org/10.1038/s41368-020-0084-8.

[7] Haddad RI, Harrington K, Tahara M, Ferris RL, Gillison M, Fayette J, *et al*. Nivolumab Plus Ipilimumab Versus EXTREME Regimen as First-Line Treatment for Recurrent/Metastatic Squamous Cell Carcinoma of the Head and Neck: The Final Results of CheckMate 651. Journal of Clinical Oncology: Official Journal of the American Society of Clinical Oncology. 2023; 41: 2166–2180. https://doi.org/10.1200/JCO.22.00332.

[8] Li S, Yu W, Xie F, Luo H, Liu Z, Lv W, *et al*. Neoadjuvant therapy with immune checkpoint blockade, antiangiogenesis, and chemotherapy for locally advanced gastric cancer. Nature Communications. 2023; 14: 8. https://doi.org/10.1038/s41467-022-35431-x.

[9] Ferris RL, Lenz HJ, Trotta AM, García-Foncillas J, Schulten J, Audhuy F, *et al*. Rationale for combination of therapeutic antibodies targeting tumor cells and immune checkpoint receptors: Harnessing innate and adaptive immunity through IgG1 isotype immune effector stimulation. Cancer Treatment Reviews. 2018; 63: 48–60. https://doi.org/10.1016/j.ctrv.2017.11.008.

[10] Mellman I, Chen DS, Powles T, Turley SJ. The cancer-immunity cycle: Indication, genotype, and immunotype. Immunity. 2023; 56: 2188–2205. https://doi.org/10.1016/j.immuni.2023.09.011.

[11] Li MO, Wolf N, Raulet DH, Akkari L, Pittet MJ, Rodriguez PC, *et al*. Innate immune cells in the tumor microenvironment. Cancer Cell. 2021; 39: 725–729. https://doi.org/10.1016/j.ccell.2021.05.016.

[12] Hashimoto A, Sarker D, Reebye V, Jarvis S, Sodergren MH, Kossenkov A, *et al.* Upregulation of C/EBPα Inhibits Suppressive Activity of Myeloid Cells and Potentiates Antitumor Response in Mice and Patients with Cancer. Clinical Cancer Research. 2021; 27: 5961–5978. https://doi.org/10.1158/1078-0432.CCR-21-0986.

[13] Goossens P, Rodriguez-Vita J, Etzerodt A, Masse M, Rastoin O, Gouirand V, *et al*. Membrane Cholesterol Efflux Drives Tumor-Associated Macrophage Reprogramming and Tumor Progression. Cell Metabolism. 2019; 29: 1376–1389.e4. https://doi.org/10.1016/j.cmet.2019.02.016.

[14] Li J, Wu C, Hu H, Qin G, Wu X, Bai F, *et al*. Remodeling of the immune and stromal cell compartment by PD-1 blockade in mismatch repair-deficient colorectal cancer. Cancer Cell. 2023; 41: 1152–1169.e7. https://doi.org/10.1016/j.ccell.2023.04.011.

[15] Zhuang X, Zhang H, Li X, Li X, Cong M, Peng F, *et al*. Differential effects on lung and bone metastasis of breast cancer by Wnt signalling inhibitor DKK1. Nature Cell Biology. 2017; 19: 1274–1285. https://doi.org/10.1038/ncb3613.

[16] Liu X, Wang J, Boyer JA, Gong W, Zhao S, Xie L, *et al*. Histone H3 proline 16 hydroxylation regulates mammalian gene expression. Nature Genetics. 2022; 54: 1721–1735. https://doi.org/10.1038/s41588-022-01212-x.

[17] D'Amico L, Mahajan S, Capietto AH, Yang Z, Zamani A, Ricci B, *et al*. Dickkopf-related protein 1 (Dkk1) regulates the accumulation and function of myeloid derived suppressor cells in cancer. The Journal of Experimental Medicine. 2016; 213: 827–840. https://doi.org/10.1084/jem.20150950.

[18] Zhai J, Chen H, Wong CC, Peng Y, Gou H, Zhang J, *et al*. ALKBH5 Drives Immune Suppression Via Targeting AXIN2 to Promote Colorectal Cancer and Is a Target for Boosting Immunotherapy. Gastroenterology. 2023; 165: 445–462. https://doi.org/10.1053/j.gastro.2023.04.032.

[19] Hegde S, Leader AM, Merad M. MDSC: Markers, development, states, and unaddressed complexity. Immunity. 2021; 54: 875–884. https://doi.org/10.1016/j.immuni.2021.04.004.

[20] Tesi RJ. MDSC; the Most Important Cell You Have Never Heard

Of. Trends in Pharmacological Sciences. 2019; 40: 4–7. https://doi.org/10.1016/j.tips.2018.10.008.

[21] Shi T, Zhang Y, Wang Y, Song X, Wang H, Zhou X, *et al*. DKK1 Promotes Tumor Immune Evasion and Impedes Anti-PD-1 Treatment by Inducing Immunosuppressive Macrophages in Gastric Cancer. Cancer Immunology Research. 2022; 10: 1506–1524. https://doi.org/10.1158/2326-6066.CIR-22-0218.

[22] Haas MS, Kagey MH, Heath H, Schuerpf F, Rottman JB, Newman W. mDKN-01, a Novel Anti-DKK1 mAb, Enhances Innate Immune Responses in the Tumor Microenvironment. Molecular Cancer Research: MCR. 2021; 19: 717–725. https://doi.org/10.1158/1541-7786.MCR-20-0799.

[23] Ye X, Liu J, Quan R, Lu Y, Zhang J. DKK1 affects survival of patients with head and neck squamous cell carcinoma by inducing resistance to radiotherapy and immunotherapy. Radiotherapy and Oncology: Journal of the European Society for Therapeutic Radiology and Oncology. 2023; 181: 109485. https://doi.org/10.1016/j.radonc.2023.109485.

[24] Klempner SJ, Sonbol MB, Wainberg ZA, Uronis HE, Chiu VK, Scott AJ, *et al*. DKN-01 in Combination With Tislelizumab and Chemotherapy as First-Line Therapy in Advanced Gastric or Gastroesophageal Junction Adenocarcinoma: DisTinGuish. Journal of Clinical Oncology: Official Journal of the American Society of Clinical Oncology. 2025; 43: 339–349. https://doi.org/10.1200/JCO.24.00410.

[25] Lee KW, Mahalingam D, Shim BY, Kim IH, Oh DY, Uronis H, *et al*. DKN-01 and tislelizumab as second-line therapy in DKK1-high gastroesophageal adenocarcinoma: DisTinGuish trial part B. Nature Communications. 2025; 16: 6393. https://doi.org/10.1038/s41467-025-61420-x.

[26] Dao V, Yuki K, Lo YH, Nakano M, Kuo CJ. Immune organoids: from tumor modeling to precision oncology. Trends in Cancer. 2022; 8: 870–880. https://doi.org/10.1016/j.trecan.2022.06.001.

[27] Raghavan S, Winter PS, Navia AW, Williams HL, DenAdel A, Lowder KE, *et al*. Microenvironment drives cell state, plasticity, and drug response in pancreatic cancer. Cell. 2021; 184: 6119–6137.e26. https://doi.org/10.1016/j.cell.2021.11.017.

[28] Bar-Ephraim YE, Kretzschmar K, Clevers H. Organoids in immunological research. Nature Reviews. Immunology. 2020; 20: 279–293. https://doi.org/10.1038/s41577-019-0248-y.

[29] Chi H, Xie X, Yan Y, Peng G, Strohmer DF, Lai G, *et al*. Natural killer cell-related prognosis signature characterizes immune landscape and predicts prognosis of HNSCC. Frontiers in Immunology. 2022; 13: 1018685. https://doi.org/10.3389/fimmu.2022.1018685.

[30] Wang R, Zhang G, Zhu X, Xu Y, Cao N, Li Z, *et al*. Prognostic Implications of LRP1B and Its Relationship with the Tumor-Infiltrating Immune Cells in Gastric Cancer. Cancers. 2023; 15: 5759. https://doi.org/10.3390/cancers15245759.

[31] Liu Z, Zhang Z, Zhang Y, Zhou W, Zhang X, Peng C, *et al*. Spatial transcriptomics reveals that metabolic characteristics define the tumor immunosuppression microenvironment via iCAF transformation in oral squamous cell carcinoma. International Journal of Oral Science. 2024; 16: 9. https://doi.org/10.1038/s41368-023-00267-8.

[32] Fan Z, Yu B, Pan T, Li F, Li J, Hou J, *et al*. DKK1 as a robust predictor for adjuvant platinum chemotherapy benefit in resectable pStage II-III gastric cancer. Translational Oncology. 2023; 27: 101577. https://doi.org/10.1016/j.tranon.2022.101577.

[33] Taube JM, Roman K, Engle EL, Wang C, Ballesteros-Merino C, Jensen SM, *et al*. Multi-institutional TSA-amplified Multiplexed Immunofluorescence Reproducibility Evaluation (MITRE) Study. Journal for Immunotherapy of Cancer. 2021; 9: e002197. https://doi.org/10.1136/jitc-2020-002197.

[34] Yin Y, Zeng A, Abuduwayiti A, Xu Z, Chen K, Wang C, *et al*. MAIT cells are associated with responsiveness to neoadjuvant immunotherapy in COPD-associated NSCLC. Cancer Medicine. 2024; 13: e7112. https://doi.org/10.1002/cam4.7112.

[35] Kansal V, Burnham AJ, Kinney BLC, Saba NF, Paulos C, Lesinski GB, *et al*. Statin drugs enhance responses to immune checkpoint blockade in head and neck cancer models. Journal for Immunotherapy of Cancer. 2023; 11: e005940. https://doi.org/10.1136/jitc-2022-005940.

[36] Parikh A, Shin J, Faquin W, Lin DT, Tirosh I, Sunwoo JB, *et al*. Malignant cell-specific CXCL14 promotes tumor lymphocyte infiltration in oral cavity squamous cell carcinoma. Journal for Immunotherapy of Cancer. 2020; 8: e001048. https://doi.org/10.1136/jitc-2020-001048.

[37] Xu J, Liu H, Wang T, Wen Z, Chen H, Yang Z, *et al*. CCR7 Mediated Mimetic Dendritic Cell Vaccine Homing in Lymph Node for Head and Neck Squamous Cell Carcinoma Therapy. Advanced Science (Weinheim, Baden-Wurttemberg, Germany). 2023; 10: e2207017. https://doi.org/10.1002/advs.202207017.

[38] Anandappa AJ, Wu CJ, Ott PA. Directing Traffic: How to Effectively Drive T Cells into Tumors. Cancer Discovery. 2020; 10: 185–197. https://doi.org/10.1158/2159-8290.CD-19-0790.

[39] Liu NN, Yi CX, Wei LQ, Zhou JA, Jiang T, Hu CC, *et al*. The intratumor mycobiome promotes lung cancer progression via myeloid-derived suppressor cells. Cancer Cell. 2023; 41: 1927–1944.e9. https://doi.org/10.1016/j.ccell.2023.08.012.

[40] Yang C, Qu L, Wang R, Wang F, Yang Z, Xiao F. Multi-layered effects of Panax notoginseng on immune system. Pharmacological Research. 2024; 204: 107203. https://doi.org/10.1016/j.phrs.2024.107203.